Post-Motor-Failure Performance of a Robust Feedback Controller for a UAM-Scale Hexacopter

Matthew Bahr
Graduate Research Assistant

Michael McKay
Graduate Research Assistant

Robert Niemiec
Research Scientist

Farhan Gandhi
Redfern Professor and MOVE Director

Center for Mobility with Vertical Lift (MOVE)
Rensselaer Polytechnic Institute
Troy, NY, United States

ABSTRACT

The performance of two flight controllers is compared for a 1200 lb hexacopter following single rotor failure. A nominal flight controller is tuned to meet handling qualities specifications for the healthy aircraft in forward flight, and a robust two-plant controller is tuned to also satisfy the same set of handling qualities specifications following front rotor failure. This two-plant controller is tuned to simultaneously meet the handling qualities for the healthy and failed aircraft. In both cases, the flight controllers do not utilize knowledge of the rotor failure. The performance of the controllers is compared for single rotor failures of the front and side rotors. For front rotor failures, the two plant controller decreases the peak pitch deviation by 3.5° and provides a more well damped response, but does not provide significant benefit during side rotor failure. Various maneuvers are also performed for each controller to evaluate the cost for using the robust controller in normal operation. The largest torque difference, a pitch doublet, requires 8 ft-lb additional torque for the two-plant controller, while the peak torque requirement for maneuvers occurs during a yaw rate step, where about 140 ft-lb of torque is required for the nominal controller (143 ft-lb for the two-plant). For both controllers, recovery following rotor failure requires substantially more torque (280 ft-lb) than the different maneuvers considered. Therefore, motor sizing is limited by rotor failure cases, not normal operation.

NOTATION

Symbols

A	Aircraft State Matrix
B	Aircraft Input Matrix
C	Output Matrix
D	Feedforward Matrix
i	Motor Current
I	Aircraft Inertia
K_e	Motor back-EMF Constant
K_t	Motor Torque Constant
p, q, r	Body Angular Rates
R_a	Motor Resistance
Q	Motor Torque
$\vec{u}$	Input Vector
u, v, w	Body Velocities
V	Motor Voltage
$\vec{x}$	State Vector
$\dot{\vec{x}}$	State Derivative Vector
$\vec{y}$	Output Vector
ϕ, θ, ψ	Roll, Pitch, Yaw Attitudes
Ω	Rotor Speed

Acronyms

ACAH	Attitude Command Attitude Hold
eVTOL	Electric Vertical Takeoff and Landing
RMAC	Rensselaer Multicopter Analysis Code
TRC	Translational Rate Command
UAM	Urban Air Mobility
VTOL	Vertical Takeoff and Landing

INTRODUCTION

The Urban Air Mobility (UAM) challenge seeks to revolutionize urban transportation by significantly decreasing transit times in urban settings. In order for UAM to become a mainstay of urban mobility, aircraft will not only need to meet commercial certifications, but also be accepted by the public at large. Safety is paramount to ensuring acceptance from the general public. Therefore, the aircraft that fill this new space must be robust to rotor degradation and failure.

Evaluation of component failure is a common and necessary step in certification and testing of various aircraft configurations. This is especially important for vehicles intended for UAM, given the increased potential for collateral damage due to the proposed operating environment and volume of operations the aircraft will be expected to perform. Two common approaches exist for fault compensation, adaptive and robust

Presented at the Vertical Flight Society's 77th Annual Forum & Technology Display, Virtual, May 10–14, 2021.

control. Adaptive control techniques require knowledge (or identification) of the fault to be able to apply fault compensation via control reallocation or gain scheduling. Some methods for detecting rotor degradation and failure in multicopters is discussed in Refs. 1 and 2. A small scale hexacopter in the presence of atmospheric turbulence is evaluated by Dutta et al. (Ref. 1). In that study statistical learning methods are employed to identify rotor degradation and failure of various rotors. Using other fault identification techniques, Frangenberg et al. (Ref. 2) goes a step further by reallocating the multicopter controls mid-flight to compensate for rotor failure. Other methods for control re-allocation are presented and discussed in Refs. 3–5. The control allocation methods presented in those studies successfully compensate for rotor faults, however, those methods require knowledge of the fault or failure in order to be implemented.

While possessing the ability to identify and detect faults is desirable, it is not always attainable. In systems where fault detection is not achievable, other strategies for failure compensation must be utilized. This is where the use of robust controllers can be beneficial, as explicit knowledge of the fault is not required to compensate for failure. Robust control techniques have previously been applied to traditional rotorcraft subject to actuator failure. One such example, by Vayalali et al. (Ref. 6), considers failure of a swashplate servo on a fully compounded UH-60. It was found that use of the horizontal stabilator for longitudinal control provides Level 1 handling qualities both before and after failure. By modifying the control mixer to use the horizontal stabilator at all times the need to identify faults was eliminated, therefore providing robust control.

Single rotor failure has been examined in detail on a small scale hexacopter by McKay et al. (Ref. 7). The focus of that study was to evaluate the performance of a feedback controller following single rotor failure during various flight conditions. The rigid body and rotor speed responses were used to quantify how a robust feedback controller responded to rotor failure. Overall, the study showed that the controller was capable of stabilizing the aircraft after single rotor failure. However, the flight controller implemented was not designed to meet any handling qualities specifications.

When designing flight controllers for larger scale multicopters (intended for UAM) it is necessary to consider established handling qualities requirements, such as those defined by ADS-33E-PRF (Ref. 8). Control design approaches led by handling qualities requirements have been implemented in recent studies on multicopters in healthy operation. Walter et al. (Ref. 9) tuned inner and outer loop flight controllers for quadcopters of various sizes, where the handling qualities requirements were scaled with aircraft size, and Bahr et al. (Ref. 10), designed flight controllers for multicopters with fixed gross weight and different numbers of rotors. Both studies examined the motor requirements for the aircraft subject to various maneuvers and discrete gusts.

The present study will apply the control design techniques used in Refs. 9 and 10 to design flight controllers robust to single rotor failure on a 1200 lb hexacopter. Flight controllers will be designed considering stability, handling qualities, and performance requirements for both the healthy and failed aircraft in forward flight. A nominal controller is tuned to meet Level 1 handling qualities for the healthy aircraft, and a robust (two-plant) controller is tuned to meet Level 1 handling qualities on the healthy and single rotor failure aircraft simultaneously. The cost associated with the robust, two-plant, controller will be evaluated by examining the torque requirements to recover the aircraft post failure, as well as to perform various maneuvers on the healthy aircraft.

AIRCRAFT MODEL

The aircraft modeled in this study is an edge-first hexacopter, shown in Fig. 1 (it is also the hexacopter modeled in Ref. 10). The aircraft has a gross weight of 1200 lb and the boom lengths are sized to maintain a 10% rotor tip-to-tip clearance. The aircraft parameters are given in Table 1.

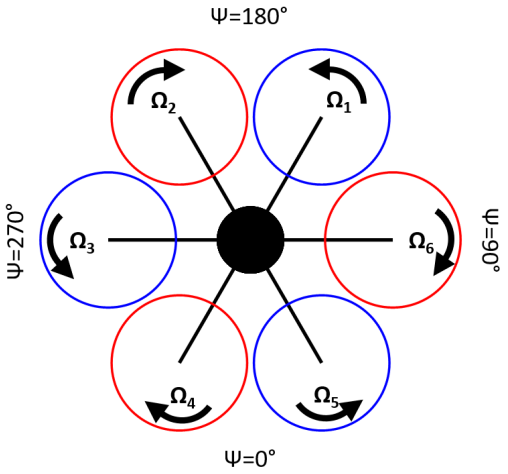

Figure 1: Hexacopter

Table 1: Hexacopter Parameters

Parameter	Value
Gross Weight	1200 lb
Disk Loading	6 psf
Rotor Radius	3.27 ft
Total Disk Area	200 ft^2
Rotor Root Pitch	21.5°
Rotor Twist	-10.4°
Tip Clearance	0.1R
Boom Length	6.86 ft
I_{xx}	370 slug ft^2
I_{yy}	431 slug ft^2
I_{zz}	719 slug ft^2

The flight dynamics are modeled using the Rensselaer Multicopter Analysis Code (RMAC, Ref. 11), which calculates aircraft accelerations by summation of forces and moments at the

aircraft center of gravity. The forces and moments produced by the rotor are calculated using blade element theory and a 3x4 Peters-He finite-state dynamic wake model (Ref. 12). RMAC is used to trim the aircraft and generate linear models to use in control optimization.

Since the aircraft is not fully controllable (but is stabilizable) following single rotor failure in hover (Ref. 13) all evaluation will be done at an airspeed of 30 knots. The flight controllers are tuned on the aircraft linearized at this airspeed, maneuvers using the healthy aircraft and nonlinear failure simulations are also performed at this airspeed. The aircraft trim result is presented in Table 2.

Table 2: Trim Parameters

Trim Parameter	Value
Airspeed	30 kt
θ	-2.60°
$V_{1,2}$	103 V
$V_{3,6}$	107 V
$V_{4,5}$	112 V
$\Omega_{1,2}$	1195 RPM
$\Omega_{3,6}$	1240 RPM
$\Omega_{4,5}$	1290 RPM
$i_{1,2}$	92.5 A
$i_{3,6}$	101 A
$i_{4,5}$	109 A

Rotor Failure

In the present study, rotor failure is represented in different ways for the linear and nonlinear models. The linearized state-space model is represented as

$$\begin{aligned} \dot{\vec{x}} &= A\vec{x} + B\vec{u}. \\ \vec{y} &= C\vec{x} + D\vec{u}. \end{aligned} \tag{1}$$

The A and B matrices take the form

$$a_{ij} = \frac{\delta \dot{x}_i}{\delta x_j},\ b_{ij} = \frac{\delta \dot{x}_i}{\delta u_j}, \tag{2}$$

With $A \in \mathbb{R}^{n\times n}$ and $B \in \mathbb{R}^{m\times n}$, where n is the number of states, and m is the number of inputs. The full state vector is comprised of the 12 rigid body states, 60 inflow states (10 per rotor), and six rotor speeds. Static condensation is performed to reduce out the inflow states from the A matrix, as performed in Ref. 7. This reduces the size of the A matrix from 72×72 to 18×18, ($C = I_{18},\ D = \mathbf{0}_{18}$).

The condensed state vector is composed of the rigid body states and rotor speeds, and the input vector is the individual motor voltages, as shown in Eqs. 3 and 4

$$\vec{x} = \{x\ \ y\ \ z\ \ \phi\ \ \theta\ \ \psi\ \ u\ \ v\ \ w\ \ p\ \ q\ \ r\ \ \vec{\Omega}\}, \tag{3}$$

$$\vec{\Omega} = \{\Omega_1\ \ \Omega_2\ \ \Omega_3\ \ \Omega_4\ \ \Omega_5\ \ \Omega_6\},$$

$$\vec{u} = \{V_1\ \ V_2\ \ V_3\ \ V_4\ \ V_5\ \ V_6\}. \tag{4}$$

To model rotor failure, the aircraft is linearized using the failed trim state, which causes the partition of the A matrix corresponding to inflow to no longer be full rank. To perform static condensation, this partition of the A matrix must be inverted, to resolve this issue the rows and columns corresponding to the failed rotor are neglected. Static condensation can then be performed, which results in the condensed A matrix missing the row and column corresponding to the failed rotor, the A matrix is 17×17. To resolve this, a row and column of zeros is inserted at the index of the failed rotor. Similarly, the condensed B matrix for the failed aircraft needs a column of zeros inserted at the index of the failed rotor.

During the nonlinear simulations, rotor failure is modeled by inputting and holding the failed motor voltage at zero volts. The zero voltage input will cause the failed rotor to slow down over some transient due to the rotor inertia. This failed rotor will continue to produce forces and moments as long as the rotor is spinning faster than 10% its nominal value. As forces nominally scale with Ω^2, a rotor below this speed produces less than 1% nominal forces.

CONTROL ARCHITECTURE

The controller used in this study is similar in architecture to the controller used in Ref. 10, and is presented in Fig. 2. The explicit model following (EMF) controller features PID feedback controllers with feedforward paths using the inverse aircraft model. The inverse plant is defined using the linearized healthy aircraft in hover.

Included within the inverse motor model block in Fig. 2 is the rotor speed command model. Tuning the rotor speed time constant will determine how quickly the rotors speed up or slow down to meet commanded rotor speeds, with a smaller time constant commanding the rotors to respond quicker (improving handling qualities specifications). However this comes at the cost of increased actuator effort.

Both the longitudinal and lateral axes operate using an attitude-command-attitude-hold (ACAH) response type. The yaw axis is rate-command-direction-hold (RCDH), while the heave axis follows a translational-rate-command (TRC) response type.

Since the yaw axis is regulated by motor torque (yaw is independent of rotor thrust) the rotor speed dynamics are not present in the yaw inverse model. Due to this, back-EMF compensation is required for yaw (additional voltage is required to compensate the changes in rotor speed), and is implemented in within the feedback controller.

Additional back-EMF compensation is applied using the reactionless rotor speed modes (Ω_{2s}, Ω_{2c}) (Ref. 14). Application of back-EMF compensation for these higher order modes is necessary to meet model following specifications for the failed aircraft, and is applied just upstream of the plant. In normal operation these rotor speed modes are not excited, however after failure, loss of a rotor causes these modes to be excited.

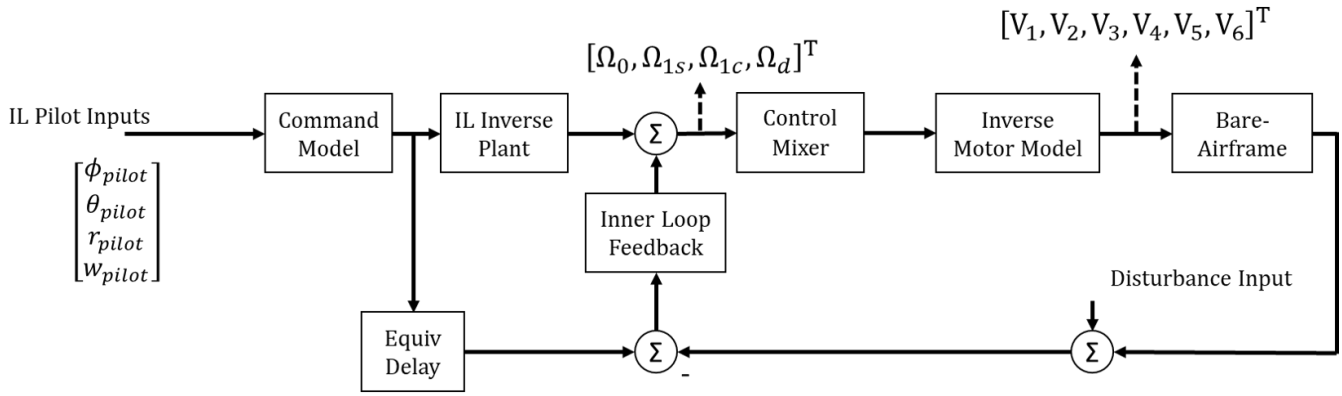

Figure 2: Control Architecture

CONTROL OPTIMIZATION METHOD

The control optimization tool CONDUIT® (Ref. 15) is used to tune flight controllers for the healthy and failed aircraft. Both flight controllers are tuned to meet a set of hard constraints, soft constraints, and performance specifications defined by ADS-33E-PRF (Ref. 8) and presented in Table 3.

Table 3: Handling Qualities Specifications

Specification	Axes
Hard Constraints	
Eigenvalues	All
Stability Margins	All
Nichols Margins	All
Soft Constraints	
Pitch Bandwidth	Pitch
Roll Bandwidth	Roll
Yaw Bandwidth	Yaw
Crossover Frequency	All
Disturbance Rej. Bandwidth	All
Disturbance Rej. Peak	All
Heave Mode Pole	Heave
Closed Loop Damping Ratio	All
Model Following	All
OLOP (Pilot)	All
OLOP (Disturbance)	All
Summed Objectives	
Actuator RMS (Pilot)	All
Actuator RMS (Disturbance)	All
Crossover Frequency	All

The handling qualities specifications listed in Table 3 are the same as the hover specifications used in Ref. 10. This set of specifications is applicable in the hover/low-speed (less than 45 knots) region of operation, which is where this aircraft is operating.

Initially, a flight controller is tuned for the healthy aircraft at an airspeed of 30 knots. This controller will be referred to as the *nominal controller*. To tune a controller for the failed aircraft, a "two-plant" optimization approach is taken. This approach evaluates the handling qualities specifications for the healthy and failed aircraft simultaneously, which ensures the controller tuned for the failed aircraft will meet Level 1 handling qualities for both the healthy and failed aircraft, and is referred to as the *two-plant controller*. The resulting gains for both flight controllers are presented in Table 4, and the differences between the controllers (and effect on the aircraft response) will be discussed in further sections.

Table 4: Nominal and Two-Plant Controllers

Controller Parameter	Nominal	Two-Plant
Roll Derivative Gain	47.4	33.4
Roll Proportional Gain	56.9	56.6
Roll Command Model Freq.	1.56	1.59
Pitch Derivative Gain	38.4	96.4
Pitch Proportional Gain	44.2	53.3
Pitch Command Model Freq.	1.25	1.39
Yaw Derivative Gain	310	319
Yaw Time Constant	0.56	0.59
Heave Derivative Gain	14.1	29.4
Heave Time Constant	3.94	4.55
Rotor Speed Time Constant	0.1	0.085

RESULTS

Handling Qualities

Controllers are tuned to meet Level 1 handling qualities for a healthy aircraft and aircraft subject to rotor 1 failure. From this, four combinations of controller and aircraft exist, two controllers and two aircraft states.

Figure 3 shows the pitch bandwidth and phase delay for the different controller and aircraft cases. Initially, for the healthy aircraft and nominal controller, the pitch bandwidth sits on the Level 1/2 boundary, as expected for an optimized controller. After failure, if the nominal controller is used, the pitch bandwidth falls into Level 2, seen as the red 'o' moving to the red 'x'. However, if the two-plant controller is used, the pitch bandwidth for the failed aircraft returns to the Level 1/2

Table 5: Handling Qualities Specs, Before and After Failure

	Healthy Aircraft Nominal Controller	Healthy Aircraft Two-Plant Controller	Rotor 1 Failure Nominal Controller	Rotor 1 Failure Two-Plant Controller
Pitch Bandwidth [rad/s]	2.00	2.24	1.56	2.00
Model Following	38	18	375	82
Closed Loop Damping Ratio	0.46	0.42	0.24	0.45

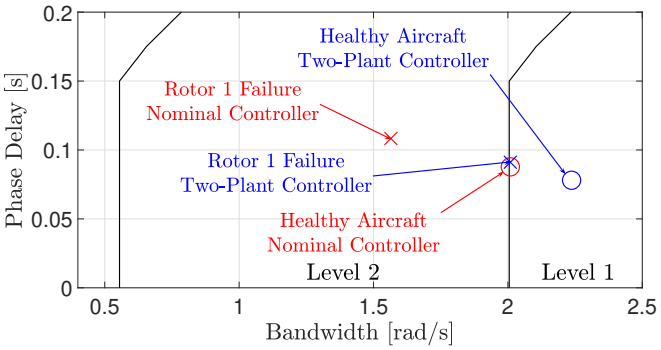

Figure 3: Pitch Bandwidth Specification

boundary, represented by the blue 'x'. For the healthy aircraft, the two plant controller pushes the pitch bandwidth deeper into Level 1 (blue 'o'), providing some additional margin in normal operation.

The pitch model following and worst closed loop damping ratios are shown in Figs. 4 and 5, respectively. Using both controllers, the healthy aircraft meets Level 1 HQ for both pitch model following and closed loop damping ratio (due to the two-plant optimization method). If the nominal controller is used following rotor 1 failure, the pitch model following drops into Level 3 (evaluating to a cost of 375). However, the two-plant controller is able to bring the pitch model following into Level 2 (cost of 82). It is possible to recover Level 1 model following by further decreasing the rotor speed time constant (making the rotors respond more aggressively).

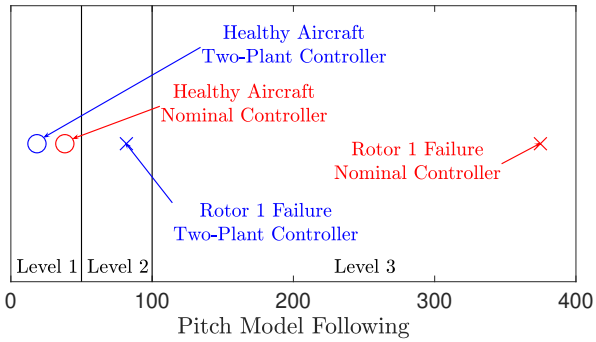

Figure 4: Pitch Model Following

The closed loop damping ratio also falls to Level 2 if the nominal controller is used post failure. The two-plant controller is able to return the failed aircraft to the same closed loop damping ratio as the healthy aircraft with nominal controller, seen in Fig. 5.

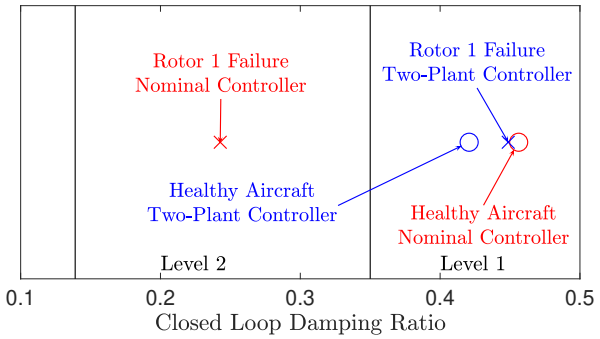

Figure 5: Worst Closed Loop Damping Ratio

Rotor Failure Simulations

Flight simulations are performed evaluating single rotor failure of rotors 1, 2, 3, and 6 (front and side rotors, Fig. 1), and the response of the aircraft is compared when using the nominal and two plant controllers. Figures 6-9 show the attitude response of the aircraft following the failures of various rotors using the nominal controller. Comparing the loss of either front rotor (Fig. 6, 7) shows that the pitch response is identical, but the roll and yaw responses are flipped, due to the geometry of the vehicle (Fig. 1), and the direction of torque produced by motor 1 or 2, respectively. Clearly, the response of the aircraft to rotor 1 or 2 failure is qualitatively similar and primarily acts in the longitudinal axis.

Similarly, comparing rotor 3 and 6 failure shows a more extreme roll response (see Figs. 8, 9) compared to rotor 1 failure. Rotors 3 and 6 are the most laterally extreme rotors, and are the primary rotors for roll authority, therefore rotor 3 and 6 failure produce a significant roll response, and little to no pitch response (as they have negligible pitch authority). Failure of rotors 3 and 6 produce a qualitatively similar response primarily in the lateral axis. Of the four rotor failure cases, only rotor 1 and rotor 3 failure will be presented.

The response to rotor 1 failure using the two-plant controller is shown in Fig. 10. The two-plant controller provides a more well damped, lower amplitude pitch response, as predicted by Table 5 and Figs 4 and 5. The maximum change in attitude from trim is shown in Table 6. The two-plant controller significantly decreases the deviation in pitch by 3.5° (more than a factor of 2). However, the two-plant controller increases the peak roll response compared to the nominal controller (by 34%).

The increase in roll deviation is caused by a decrease in the roll feedback gains for the two-plant controller (Table 4). When tuning the two-plant controller, the rotor speed time

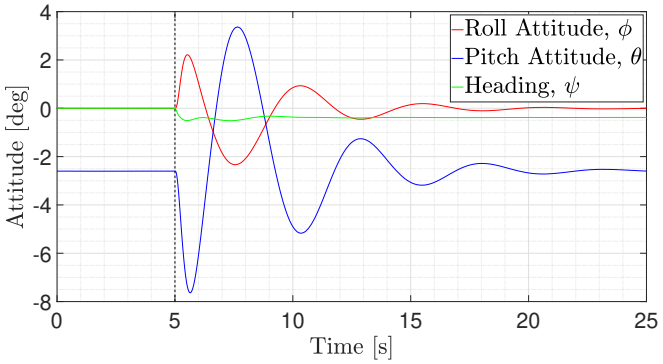

Figure 6: Rotor 1 Failure, Nominal Controller

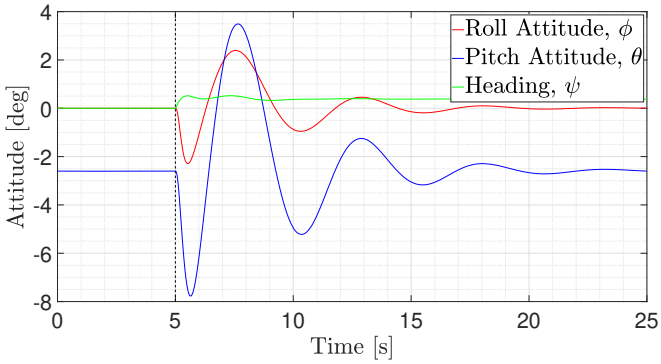

Figure 7: Rotor 2 Failure, Nominal Controller

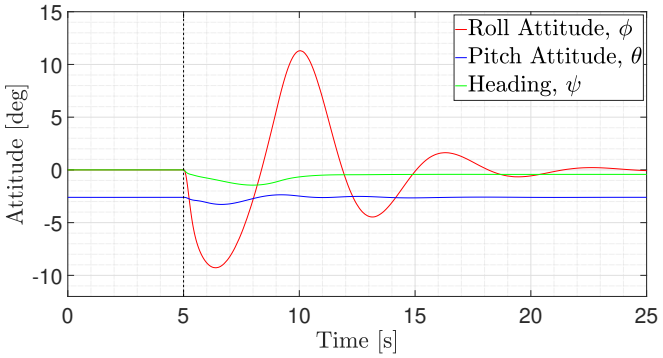

Figure 8: Rotor 3 Failure, Nominal Controller

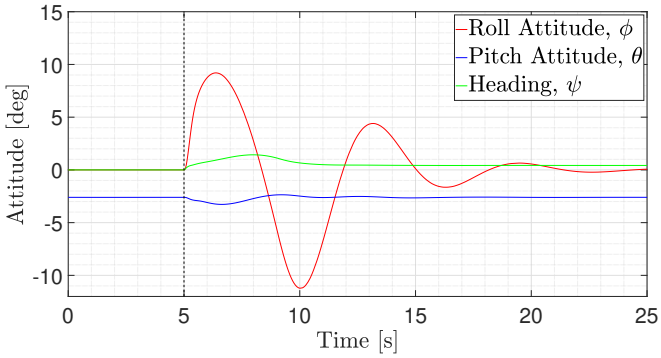

Figure 9: Rotor 6 Failure, Nominal Controller

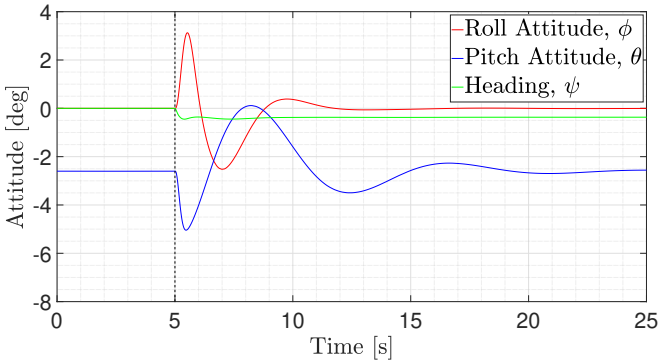

Figure 10: Rotor 1 Failure, Two-Plant Controller

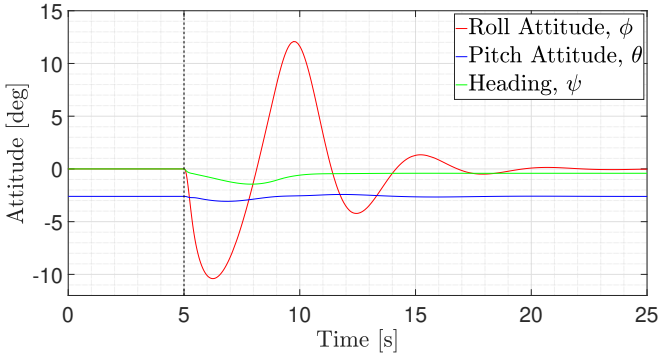

Figure 11: Rotor 3 Failure, Two-Plant Controller

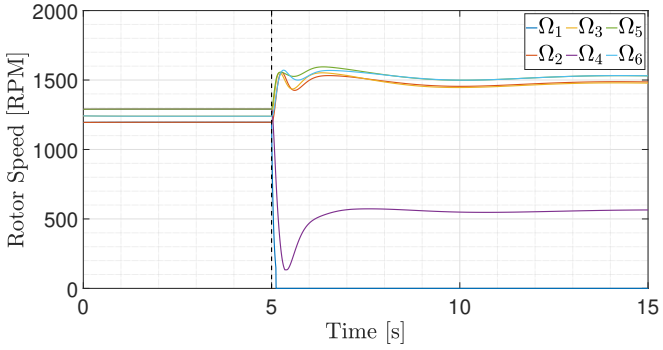

Figure 12: Rotor Speed Response to Rotor 1 Failure, Two-Plant Controller

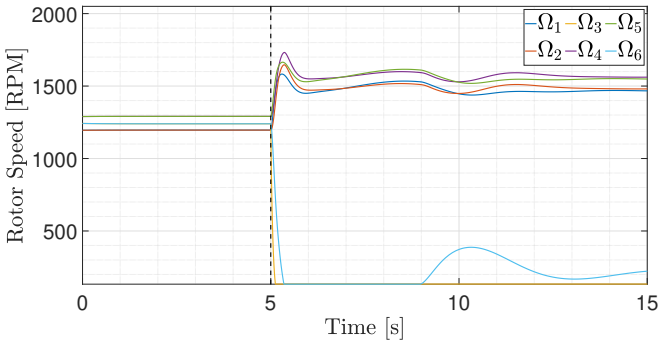

Figure 13: Rotor Speed Response to Rotor 3 Failure, Two-Plant Controller

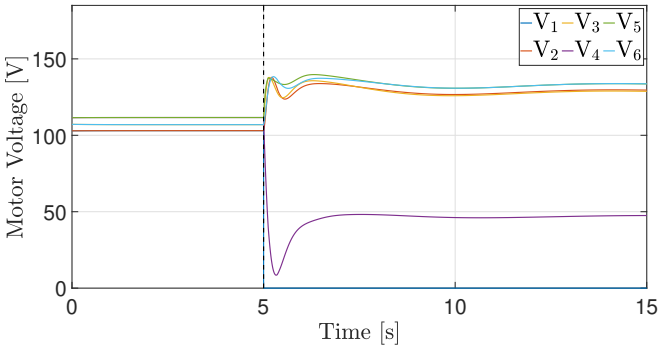

Figure 14: Voltage Response to Rotor 1 Failure, Two-Plant Controller

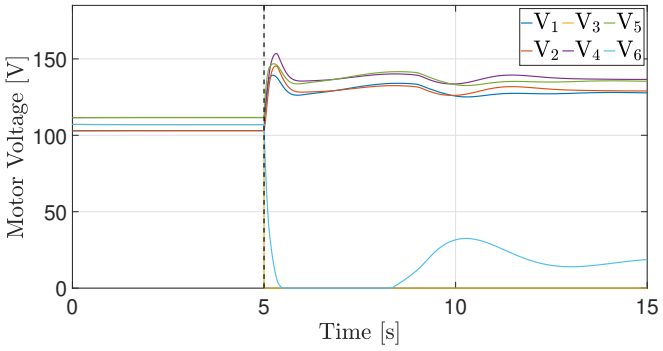

Figure 15: Voltage Response to Rotor 3 Failure, Two-Plant Controller

Table 6: Rotor 1 Failure, Max Attitude Change

	$\lvert\Delta\theta\rvert$	$\lvert\Delta\phi\rvert$
Nominal Controller	5.97°	2.34°
Two-Plant Controller	2.44°	3.13°

constant must be decreased to meet the model following requirements in pitch. This reduced time constant allows the optimization routine to decrease the roll derivative gain while maintaining stability margins in roll. A consequence of the reduction of time constant and derivative gain is an increase in the roll response, but Level 1 HQ are still met.

The two-plant controller does not provide the same benefits in the case of rotor 3 failure, shown in Figs. 8 and 11. There is not a substantial difference in vehicle response between the two controllers. Rotor 3 failure is outside of the design consideration of the two-plant controller, which is optimized to meet Level 1 handling qualities following *rotor 1 failure*. Due to this, another two-plant controller (for healthy and rotor 3 failure) or three-plant controller (healthy, rotor 1, and rotor 3 failure) could be tuned for improved performance following rotor 3 failure.

The individual rotor speed response is presented in Figs. 12 and 13 for rotor 1 and rotor 3 failure, respectively. In both cases, the response of the failed rotor is similar. At the time of failure, the voltage to the failed motor is interrupted, but the failed rotor does not immediately stop spinning due to its inertia. The rotor diametrically opposite the failed rotor significantly reduces speed to reduce the moment imbalance following failure, while the remaining rotors speed up to make up for the loss of lift from the failed rotor. In the case of rotor 1 failure (Fig. 12), rotor 4 rapidly decreases its speed and nearly stops spinning. After the aircraft recovers, rotor 4 increases in speed and settles at a steady value to maintain torque balance.

Following rotor 3 failure, rotor 6 quickly slows down, almost as fast as the failed rotor (Fig. 13). The response of rotor 6 is aggressive enough that it stops spinning entirely, stopping for about 4 seconds. Once rotor 6 starts spinning again (at 9 seconds), the remaining 4 rotors must adjust speed to compensate for the additional forces and moments produced by rotor 6.

The voltage inputs following rotor failure is shown in Figs. 14 and 15. Due to the relationship between motor voltage and rotor speed, the motor voltage response to rotor failure closely resembles the rotor speed response. The aggressive change in rotor 6 speed in the rotor 3 failure case can be explained by the respective voltage response. Figure 15 shows that zero commanded voltage to rotor 6 for a few seconds is required to stabilize the aircraft.

The peak current values in response to rotors 1 and 3 failure are tabulated in Table 7. In all failure cases, the rotor diametrically opposite the failed rotor sees the largest peak current and is negative in all cases due to the rapid decrease in both the motor voltage and rotor speed. In the case of rotor 1 failure, the two-plant controller requires a peak current of -489A to provide the response shown in Fig. 10. For further context, the equation for motor current is given by Eq. 5,

$$i = \frac{1}{R_a}(V - K_e\Omega). \tag{5}$$

The voltage drop commanded during deceleration is insufficient to overcome the back-EMF of the motor ($K_e\Omega$), and thus current flows backward through the motor (which briefly acts as a generator, similar to regenerative braking).

Table 7: Peak Current Following Rotor Failure

Failure Case	Controller	Peak Current
Rotor 1 Failure	Nominal	-424 A (Rotor 4)
	Two-Plant	-489 A (Rotor 4)
Rotor 3 Failure	Nominal	-455 A (Rotor 6)
	Two-Plant	-436 A (Rotor 6)

Aircraft Maneuvers

Various maneuvers are performed to compare the cost associated with using the two-plant controller in normal operation. Doublet maneuvers are used in the pitch and roll axes, and step commands are used in yaw and heave. The response of the vehicle to a 10° roll doublet is shown in Fig. 16. Both the nominal and two-plant controllers have similar commanded

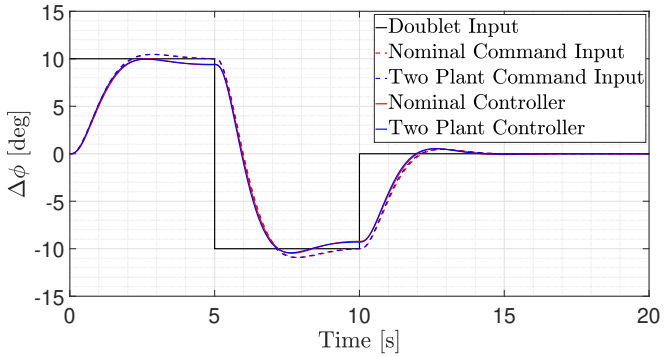

Figure 16: Roll Doublet Response

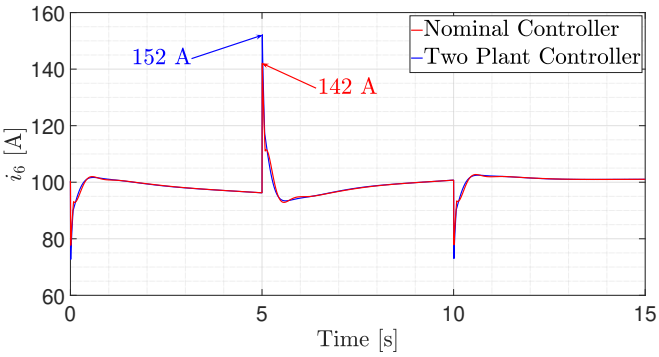

Figure 17: Roll Doublet Current Response

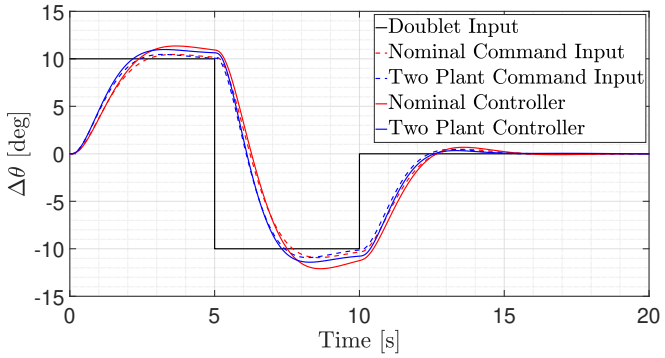

Figure 18: Pitch Doublet Response

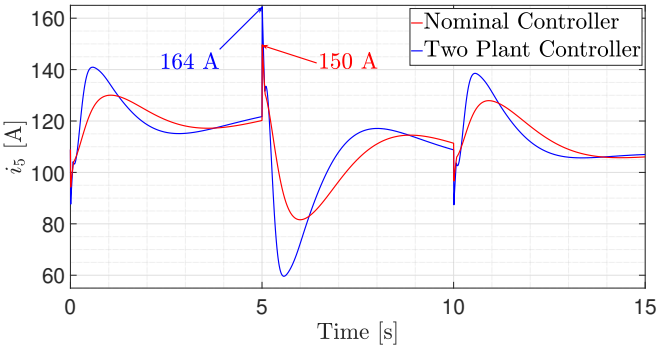

Figure 19: Pitch Doublet Current Response

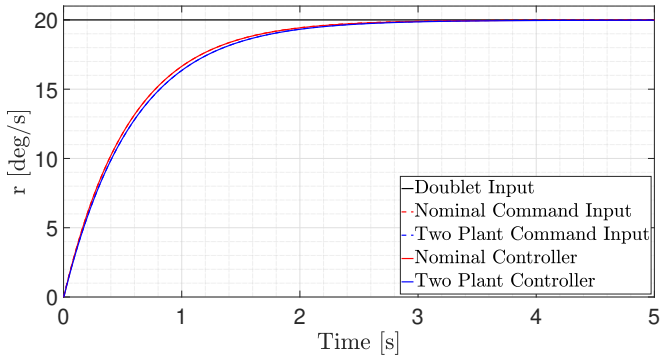

Figure 20: Yaw Rate Step Response

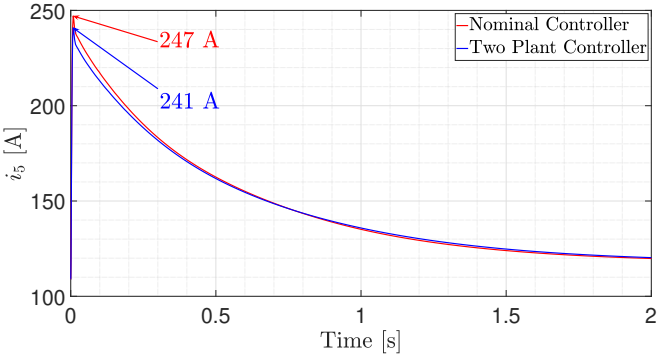

Figure 21: Yaw Rate Step Current Response

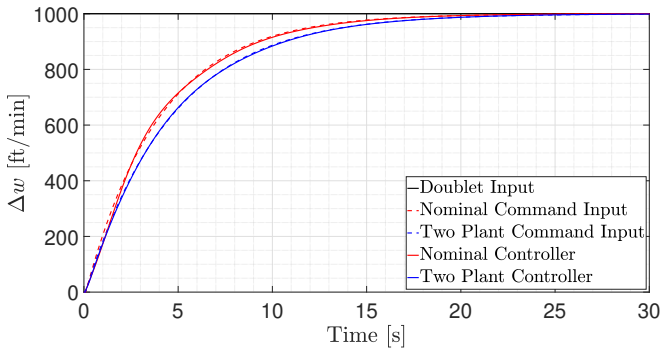

Figure 22: Heave Step Response

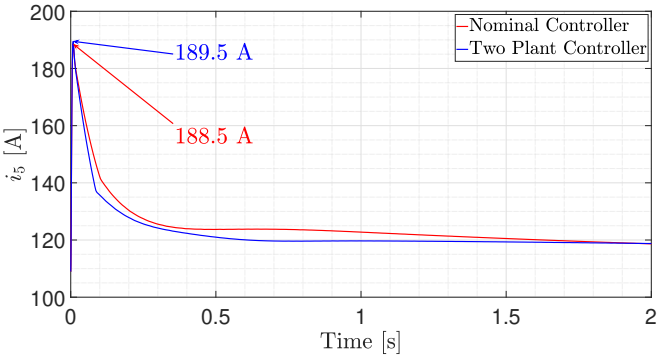

Figure 23: Heave Step Current Response

inputs and vehicle responses, due to the similar command model frequencies and feedback gains (Table 4). The corresponding current response is shown in Fig. 17, and the peak values are tabulated in Tables 8 and 9. The two-plant controller has a peak current 10A higher than the nominal controller, this is due to the smaller rotor speed time constant used by the two-plant controller.

A 10° pitch doublet is shown in Fig. 18. The difference in response in this axis is caused by the differences in command model frequency and feedback gains. Figure 18 shows that the commanded input for the two-plant controller leads the nominal controller, which is caused by the two-plant controller having a higher command model frequency (about 11% larger than the nominal controller, Table 4). This increase builds in bandwidth margin for the healthy aircraft and places the pitch bandwidth on the Level 1/2 boundary post failure (Fig. 3). The shape of the pitch response and tracking error are also noticeably different between the two controllers. In Fig. 18, at 5 seconds, the two plant controller has a smaller error (the aircraft response is closer to the commanded signal compared to the nominal controller). Over the entire pitch response, the tracking error of the two-plant controller is less than the nominal controller. These differences in aircraft response are caused by the change in feedback gains from the nominal to two-plant controllers. To meet Level 1 handling qualities the pitch derivative gain increased by 151% from the nominal to the two-plant controller and the pitch proportional gain increased by 21% (Table 4).

The current response to the pitch doublet is shown in Fig. 19. The two-plant controller requires 14A more current to follow the doublet, slightly more than the difference seen in the roll axis. This is because the two-plant controller has a more aggressive response in pitch due to the command model frequency increasing, the rotor speed time constant decreasing, and the increased aircraft inertia in pitch.

A step input of 20°/s is used to evaluate the response and actuator effort in the yaw axis. The vehicle response to the yaw step is shown in Fig. 20. Both controllers follow slightly different commanded inputs due to the different yaw time constants. However, each controller exactly follows the commanded input, with each respective solid curve sitting on top of the dashed line.

The current response to the yaw rate step is shown in Fig. 21. Immediately, there is a large surge in current to produce the differential torque required to yaw the aircraft. The peak current required for the yaw step is much greater than the requirement for the roll and pitch doublets (80-90 A greater), and is due to motor torque directly actuating the yaw axis. Both controllers require similar peak current, with the nominal controller requiring slightly more, caused by the difference in yaw command model time constant between the controllers. The yaw time constant is slightly smaller for the nominal controller (causing a more aggressive response) compared to the two-plant controller.

That last maneuver evaluated is a 1000 ft/min heave step, shown in Fig. 22. Both controllers follow the commanded signal well, with little to no deviation from the commanded input. The current response to the heave step is shown in Fig. 23. Both controllers see the same peak current, although they have different time constants. The heave step occurs over a much longer duration, causing the initial current spikes to be nearly identical. Similar to yaw, the nominal controller has a lower (and more aggressive) time constant. The effect of this lower time constant is not seen in the peak, but it is seen in the current response following the peak, where the current requirement for the nominal controller is greater than the two-plant controller for 2 seconds following the peak value.

Table 8: Nominal Controller Peak Torque from Maneuvers and Rotor Failure

	Rotor	Peak Current [A]	Peak Torque [ft-lb]
Rotor 1 Failure	Rotor 4	-424	246
Rotor 3 Failure	Rotor 6	-455	264
Roll Doublet	Rotor 6	142	82.6
Pitch Doublet	Rotor 5	150	87.0
Yaw Rate Step	Rotor 5	241	140
Heave Step	Rotor 5	188.5	109

Table 9: Two-Plant Controller Peak Torque from Maneuvers and Rotor Failure

	Rotor	Peak Current [A]	Peak Torque [ft-lb]
Rotor 1 Failure	Rotor 4	-489	284
Rotor 3 Failure	Rotor 6	-436	253
Roll Doublet	Rotor 6	152	88.5
Pitch Doublet	Rotor 5	164	95.1
Yaw Rate Step	Rotor 5	247	143
Heave Step	Rotor 5	189.5	110

Torque Requirements

An important parameter for motor sizing (and therefore aircraft design due to the relationship between motor torque and motor weight (Ref. 16) is the peak torque requirement. The peak current and calculated torque are presented in Tables 8 and 9, calculated from Eq. 6 using the torque constant from the hexacopter in Ref. 10 ($K_t = 0.79$ Nm/A), in SI units $K_e = K_t$,

$$Q = K_t i. \tag{6}$$

The peak torque requirements for the nominal controller are shown in Table 8. The rotor failure cases require much higher peak torque than the various maneuvers considered. The overall peak torque of 264 ft-lb occurs on rotor 6 for the rotor 3 failure case. In contrast, the peak torque for maneuvers is 140 ft-lb, and occurs on rotor 5 during the yaw rate step, which means the rotor failure case requires nearly twice the peak torque of the all the maneuvers.

Similarly, the peak torque requirements for the two-plant controller are shown in Table 9. For the two-plant controller, the overall peak torque occurs on rotor 4 during rotor 1 failure. In this case, rotor 4 sees a peak torque of 284 ft-lb, which is twice the peak torque seen during maneuvers.

Overall, the difference in peak torque between the two controllers is much more severe in the rotor failure cases. During a maneuver on the healthy aircraft all rotors are utilized to follow the commanded input. In contrast, when rotor failure occurs the remaining rotors must respond aggressively to stabilize the aircraft. The rotor diametrically opposite the failed rotor must change speed quickly to stabilize the aircraft, causing rotor failure cases to have the largest overall peak torque. Specifically, during rotor 1 failure the two-plant controller sees a peak torque 37 ft-lb greater than the nominal controller, the largest increase in peak torque between the controllers for different maneuvers is 8 ft-lb (for the pitch doublet).

CONCLUSIONS

Flight controllers were designed to meet handling qualities requirements on a 1200 lb hexacopter in forward flight. A nominal controller was designed for the healthy aircraft, and a robust, two-plant controller was tuned for the aircraft subject to rotor 1 failure. The handling qualities for each aircraft (healthy and rotor 1 failure) were evaluated using each controller. Following rotor 1 failure, the nominal controller is unable to meet bandwidth and model following requirements. Implementation of the two-plant controller returns the violated specifications to Level 1 for the failed aircraft. Applying the two-plant controller to the healthy aircraft pushes many of the specifications into Level 1, providing additional margin in normal operation.

Nonlinear flight simulations were run to evaluate how the two controllers perform following failure of different rotors. In all cases, the controller did not have knowledge of the fault occurring. Failure of the front rotors (rotors 1 and 2) are qualitatively similar, primarily creating a pitch response. For front rotor failure, the two-plant controller decreases the peak deviation in pitch attitude, as well as providing a more well damped response. However, the two-plant controller slightly increases the roll deviation for front rotor failure.

The two-plant controller does not provide the same benefit for side rotor failure (rotors 3 and 6), the roll response after rotor 3 failure is very similar for both the nominal and two-plant controllers. A two-plant controller for rotor 3 failure, or even a three-plant controller can be implemented to improve lateral performance following side rotor failure.

Various maneuvers were used to compare the nominal and two-plant controllers in healthy operation. In all maneuvers, the two controllers provided similar responses and current requirements. At most, the current requirement differed by 14A (for a pitch doublet), which translates to a difference of 8 ft-lb. The yaw rate step required the most current for both controllers, requiring 247A and 241A for the nominal and two-plant controllers, respectively.

In normal operation, the two-plant controller did not require significantly more motor torque compared to the nominal controller. However, the torque required to recover from single rotor failure was significantly higher (38 ft-lb, 15.4%) for the two-plant controller. The cost of the higher torque requirement provided a smaller deviation in attitude, and a more well damped response following failure.

Author contact:
Matthew Bahr: bahrm2@rpi.edu
Michael McKay: mckaym2@rpi.edu
Robert Niemiec: niemir2@rpi.edu
Farhan Gandhi: gandhf@rpi.edu

ACKNOWLEDGMENTS

This work is carried out at Rensselaer Polytechnic Institute under the Army/Navy/NASA Vertical Lift Research Center of Excellence (VLRCOE) Program, grant number W911W61120012, with Dr. Mahendra Bhagwat as Technical Monitor.

Michael McKay is supported through the National Defense Science and Engineering Graduate (NDSEG) Fellowship by the Department of Defense, Army Research Office.

REFERENCES

1. Dutta, A., McKay, M., Kapsaftopoulos, F., and Gandhi, F., "Rotor Fault Detection and Identification for a Hexacopter Based on Control and State Signals via Statistical Learning Methods," Vetrical Flight Society 76th Annual Forum & Technology Display, Virtual, October 6–8, 2020.

2. Frangenberg, M., Stephan, J., and Fichter, W., "Fast Actuator Fault Detection and Reconfiguration for Multicopters," AIAA Guidance, Navigation, and Control Conference, Kissimmee, Florida, January 5–9, 2015.

3. Marks, A., Whidborne, J., and Yamamotor, I., "Control Allocation for Fault Tolerant Control of a VTOL Octorotor," UKACC International Conference on Control, Cardiff, UK, September 3–5, 2012.

4. Achtelik, M. C., Doth, K.-M., Gurdan, D., and Stumpf, J., "Design of a Multi Rotor MAB with regard to Efficiency, Dynamics and Redundancy," AIAA Guidance, Navigation, and Control Conference, Minneapolis, Minnesota, August 13–16, 2012.

5. Falconi, G. P., Heise, C. D., and Holzapfel, F., "Novel Stability Analysis of Direct MRAC with Redundant Inputs," 24th Mediterranean Conference on Control and Automation, Athens, Greece, June 21–24, 2016.

6. Vayalali, P., McKay, M., Krishnamurthi, J., and Gandhi, F., "Robust Use of Horizontal Stabiliator in Feedback Control on a UH-60 Black Hawk," Vertical Flight Society 75th Annual Forum & Technology Display, Philadelphia, PA, May 13–16, 2019.

7. McKay, M., Niemiec, R., and Gandhi, F., "Post-Rotor-Failure Performance of a Feedback Controller for a Hexacopter," AHS International 74th Annual Forum & Technology Display, Phoenix, AZ, May 14–17, 2018.

8. "Aeronautical Design Standard, Performance Specification, Handling Qualities Requirements for Military Rotorcraft," Technical Report ADS-33E-PRF, March 2000.

9. Walter, A., McKay, M., Niemiec, R., and Gandhi, F., "Hover Handling Qualities of Fixed-Pitch, Variable-RPM Quadcopters with Increasing Rotor Diameter," Vertical Flight Society 76th Annual Forum, Virtual, October 6–8, 2020.

10. Bahr, M., McKay, M., Niemiec, R., and Gandhi, F., "Handling Qualities Assessment of Large Variable-RPM Multi-Rotor Aircraft for Urban Air Mobility,," Vertical Flight Society 76th Annual Forum, Virtual, October 6–8, 2020.

11. Niemiec, R., and Gandhi, F., "Development and Validation of the Rensselaer Multicopter Analysis Code (RMAC): A Physics-Based Comprehensive Modeling Tool," Vertical Flight Society 75th Annual Forum, Philadelphia, PA, May 12–16, 2019.

12. Peters, D., Boyd, D., and He, C. J., "Finite-State Induced-Flow Model for Rotors in Hover and Forward Flight," *Journal of the American Helicopter Society*, Vol. 34, (4), 1989, pp. 5–17.

13. Du, G.-X., Quan, Q., and Cai, K.-Y., "Controllability Analysis and Degraded Control for a Class of Hexacopters Subject to Rotor Failures," *Journal of Intelligent Robotic Systems*, Vol. 78, (1), 2015, pp. 143–157.

14. Niemiec, R., and Gandhi, F., "Multi-rotor Coordinate Transforms for Orthogonal Primary and Redundant Control Modes for Regular Hexacopters and Octocopters," 42nd Annual European Rotorcraft Forum, Lille, France, September 5–8, 2016.

15. Tischler, M., Berger, T., Ivler, C., Mohammadreza, M. H., Cheung, K. K., and Soong, J. Y., "Practical Methods for Aircraft and Rotorcraft Flight Control Design: An Optimization-Based Approach," AIAA Education Series, Reston, VA, 2017.

16. Johnson, W., "NDARC - NASA Design and Analysis of Rotorcraft," Technical Report NASA TP 218751, April 2015.